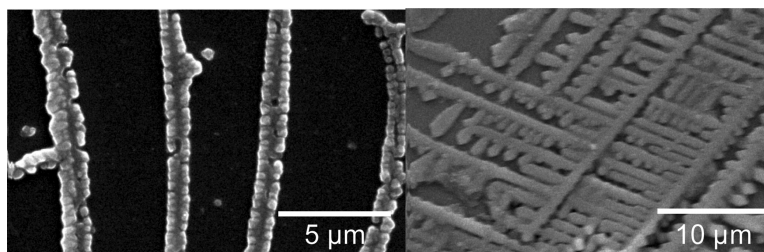


Creating Ordered Small-Scale Biologically-Based Rods through Force-Controlled Stamping

Chao-Min Cheng, and Philip R. LeDuc

J. Am. Chem. Soc., **2007**, 129 (31), 9546-9547 • DOI: 10.1021/ja072079e • Publication Date (Web): 18 July 2007

Downloaded from <http://pubs.acs.org> on February 16, 2009



More About This Article

Additional resources and features associated with this article are available within the HTML version:

- Supporting Information
- Access to high resolution figures
- Links to articles and content related to this article
- Copyright permission to reproduce figures and/or text from this article

[View the Full Text HTML](#)

Creating Ordered Small-Scale Biologically-Based Rods through Force-Controlled Stamping

Chao-Min Cheng and Philip R. LeDuc*

Departments of Mechanical and Biomedical Engineering and Biological Sciences, Carnegie Mellon University, Pittsburgh, Pennsylvania 15213

Received March 23, 2007; E-mail: prleduc@cmu.edu

The synthesis of small-scale rods has attracted significant scientific interest because of the novel structures, properties, and potential applications that could be enabled in fields such as optics, electronic nanodevice production, and chemical and biological sensor fabrication. One main concern in this field though is the ability to assemble rods at desired locations on a substrate. While some success in nanorod and nanowire devices has been recently reported, limitations in their properties and fabrication methods have greatly inhibited their scalability and development, especially in the area of high-density arrays.¹ Thus, finding novel approaches, especially those that take advantage of naturally existing biological-based methods and materials, may provide a more robust route to nanorod development. Biologically inspired and biologically based materials have properties that allow unique approaches and methodologies to be used to create ordered arrays of small-scale systems. One of these approaches is to use specific chemical reactions, which are inherently self-organized, to create new paradigms for structural and materials fabrication.² Recently, for example, a method for preparing predesigned protein–metal wires was developed based on the use of G-actin as a molecular building block. This was accomplished through the polymerization of Au-nanoparticle-functionalized G-actin monomer units and unlabeled G-actin units, resulting in the creation of metal-patterned protein filaments after catalytic metallization of the particles.³ Furthermore, biomolecules such as ATP-driven myosin movement with the actin cytoskeleton have been merged with inorganic systems to create hybrid systems that can actuate and move using small scale wire templating systems.⁴ To create and control the ordering of the polymerization of actin at defined positions on substrates would provide a tremendous advancement for fields that currently rely on mainly random occurring events within these chemical processes.

The ability to create defined patterns of materials at the nanometer scale will allow us to pursue technology and science in novel directions. One direction that has been utilized to accomplish this task is based on lithography including soft lithography, dip-pen lithography, and nanoimprinting.⁵ Lithography-based micro-contact printing using polymeric stamps such as poly(dimethylsiloxane) (PDMS) has been applied to immobilize molecules, small scale materials, and biomaterials⁶ at desired positions over large areas. In this Communication, we demonstrate a printing method that imposes a mechanical force on the upper surface of the stamp to regulate the dewetting process of the inorganic buffer, and, consequently, the evaporation rate of the solvent in this buffer. We use this to influence the characteristics of the dewetting process and the polymerization of G-actin in vitro, ultimately providing us with the ability to obtain organized filamentous actin-based nanorods in defined patterns.

Figure 1a illustrates the schematic for this microstamping process. Patterned PDMS stamps (Dow Corning) were fabricated

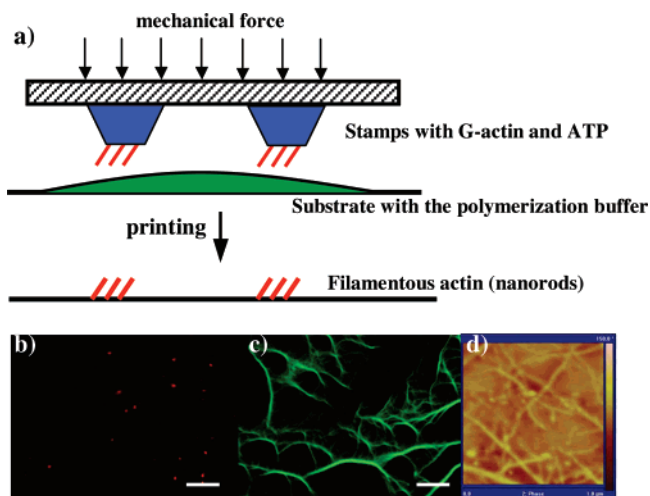


Figure 1. (a) Schematic of microstamping for forming filamentous actin nanorods achieved by polymerization of actin filaments and balancing the dewetting of an inorganic buffer and the evaporation rate of the solvent. Fluorescence images of (b) G-actin and (c) F-actin (scale bar = 1 μm). F-actin and G-actin were stained with 6 μM Alexa Fluor 488 phalloidin (Molecular Probes) and 0.3 μM D-Nase (Molecular Probes), respectively. The samples were imaged with a fluorescent microscope (Zeiss Axiovert) using a 63 \times high numerical aperture (1.4) oil immersion objective. (d) An atomic force microscope image of the matrix of F-actin in an aqueous environment with a silicon nitride tip (spring constant of a cantilever is 0.2 N/m).

using conventional soft lithography for patterning the actin filaments. The solutions for the stamping were 1 mL of ATP-buffer (general actin buffer, from *Cytoskeleton*) combined with 2 μL of ATP (100 mM). The G-actin was resuspended in the ATP-buffer for a final concentration of 0.4 mg/mL. The PDMS stamps were treated with the G-actin solution and ATP for 1 h while the glass substrate was covered with the polymerization buffer (25–150 mM KCl, 1 mM MgCl_2 and 1 mM ATP with a pH of 7.0–8.0; actin polymerization buffer from *Cytoskeleton*). The PDMS stamps were then brought into contact with the substrate at room temperature for 1 h. Figure 1b is an epifluorescent image of the G-actin in solution with D-Nase staining. Figure 1c is an image of the polymerized actin that has lengths here between 5 and 10 μm ; these were created without the application of mechanical force and labeled with phalloidin. The samples were examined under a fluorescent microscope (Zeiss Axiovert) using a 63 \times high numerical aperture oil immersion objective to image the G-actin monomer aggregates and F-actin. We also imaged the filamentous actin using an atomic force microscope (AFM). Figure 1d reveals the F-actin in an aqueous environment as viewed with the AFM. This figure shows not only the distribution of F-actin in a network, but also a higher resolution portrayal of individual F-actin on the surface of the material.

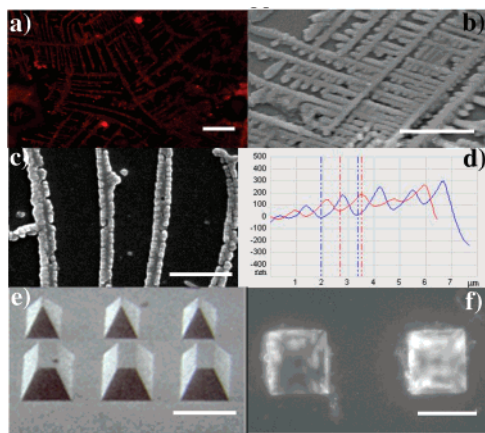


Figure 2. Pattern formation using mechanically controlled biological component printing. (a) Fluorescence (scale bar = 1 μm) and (b) SEM images (scale bar = 10 μm) of the highly regular filamentous actin nanorod array that was formed using the force-controlled microcontact printing. F-actin nanorods are the nucleation center of the organic salt crystallization. Higher magnification (c) SEM image (scale bar = 5 μm) and (d) cross-section profile (AFM) of a nanorod arrays. In panel d, the red and blue lines are the scanning results for different locations of the same sample (the y-axis is nm in height). The pattern was scanned using an atomic force microscope with a silicon nitride tip (the spring constant of the cantilever is 0.2 N/m). (e) SEM image of the PDMS mold used in this study (scale bar = 250 μm) and (f) a fluorescent image of a transferred pattern (scale bar = 50 μm).

Figure 2a and 2b display an epifluorescent image and a scanning electron microscope (SEM) image of a nanorod array when we applied a mechanical force of 0.75 N to the surface of the stamp. The dewetting process between the hydrophobic stamped (PDMS) surface and the inorganic buffer was influenced by applying a force. This influenced the polymerization of the filamentous-based nanorods which could be controlled at specific locations and with reproducible patterns (Figure 2b). Furthermore, by using this approach, we could control the nucleation center of the inorganic salt crystallization, which organized from the actin filaments. The size of the small scale rods observed in the SEM image (Figure 2c) was much larger than the known width of single actin filaments, 7 nm, as the crystallization occurred around the filaments. Figure 2d demonstrates that the F-actin rod array was a regular pattern. This regular pattern was found through the interactions between the evaporation rate of the solvent in the organic buffer and the application of mechanical force. Thus a generalized equation for this interfacial equilibrium between the liquid solvent in the buffer and vaporized solvent in the atmosphere may take the following form:

$$e = F(C_1, C_1^*) \quad (1)$$

In this equation, C_1 is the concentration of solute at the interface, C_1^* is the solvent vapor pressure at the interface, and F is a function that provides the evaporation rate.⁷ In our process, the evaporation rate of solvent in our buffer was 1 mL per 30 min when applying a mechanical force on the PDMS stamp, and 1 mL per hour without mechanical force application. Figure 2e shows a SEM image of PDMS molds and Figure 2f shows a fluorescent image of a printed pattern. When using a stamp, but not applying a continuous force as shown in Figure 3 a, the behavior of this system was governed

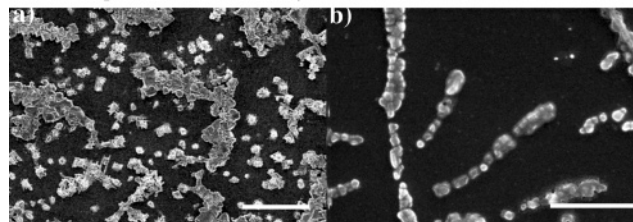


Figure 3. (a) An SEM image of the process when force is not applied. Although linear patterns are not observed here, we can form layered patterns through multiple applications of the buffered solutions (scale bar = 100 μm). (b) SEM image displaying examples of shorter nanorod length achieved by limiting total reaction time to 40 min (scale bar = 5 μm).

by the evaporation rate of the inorganic buffer; this allowed the formation of structures but they were not ordered. Furthermore, the effect of other factors, such as buffer concentration, immersion time, and total polymerization time of G-actin affected the entire process. This can be used to obtain a wider range of potential patterns as shown in Figure 3b which demonstrates that a suboptimal polymerization time led to the creation of shorter rods with the application of force.

In summary, we have developed a method to create nanorod arrays over a large area through a mechanics-based approach. By applying a manual force to a polymer stamp for biopolymers, we are able to regulate the interactions between actin, the inorganic buffer, and the substrate. This work has potential applications in a variety of fields including the study of self-organized biologically inspired material patterning, and small-scale fabrication technology.

Acknowledgment. This work was supported in part by the National Science Foundation-CAREER, National Academies Keck Foundation Futures Initiative, Pennsylvania Infrastructure Technology Alliance, the Department of Energy-Genome to Life and the Beckman Young Investigators Program (P.R.L.). C.-M. C. was supported in part by a Ph.D Research Scholarship from Taiwan and the Dowd-ICES Scholarship from Carnegie Mellon University.

References

- (1) (a) Cui, Y.; Wei, Q.; Park, H.; Lieber, C. M. *Science* **2001**, *293*, 1289–1292. (b) Kong, J.; Franklin, N. R.; Zhou, C. W.; Chapline, M. G.; Peng, S.; Cho, K. J.; Dai, H. *Science* **2000**, *287*, 622–625. (c) Li, C. Z.; He, H. X.; Bogozzi, A.; Bunch, J. S.; Tao, N. J. *Appl. Phys. Lett.* **2000**, *76*, 1333–1335. (d) Favier, F.; Walter, E. C.; Zach, M. P.; Benter, T.; Penner, R. M. *Science* **2001**, *293*, 2227–2231.
- (2) (a) Scheibel, T.; Parthasarathy, R.; Sawicki, G.; Lin, X.-M.; Jaeger, H.; Lindquist, S. L. *Proc. Natl. Acad. Sci. U.S.A.* **2003**, *100*, 4527–4532. (b) Reches, M.; Gazit, E. *Science* **2003**, *300*, 625–627. (c) Keren, K.; Krueger, M.; Gilad, R.; Ben-Yoseph, G.; Sivan, U.; Braun, E. *Science* **2002**, *297*, 72–75.
- (3) Patolsky, F.; Weizmann, Y.; Willner, I. *Nat. Mater.* **2004**, *3*, 692–695.
- (4) (a) Mehta, A. J. *Cell Sci.* **2001**, *114*, 1981–1998. (b) Yanagida, T.; Iwane, A. *Proc. Natl. Acad. Sci. U.S.A.* **2000**, *97*, 9357–9359. (c) Vale, R. D.; Milligan, R. A. *Science* **2000**, *288*, 88–95.
- (5) (a) Xia, Y.; Whitesides, G. M. *Angew. Chem., Int. Ed.* **1998**, *37*, 550–575. (b) Piner, R. D.; Zhu, J.; Xu, F.; Hong, S. H.; Mirkin, C. A. *Science* **1999**, *283*, 661–663. (c) Chou, S.; Krauss, P. R.; Renstrom, P. J. *Science* **1996**, *272*, 85–87.
- (6) (a) LeDuc, P. R.; Ostuni, E.; Whitesides, G. M.; Ingber, D. *Methods Cell Biol.* **2002**, *69*, 385–401. (b) Meitl, M. A.; Zhou, Y.; Gaur, A.; Jeon, S.; Usrey, M. L.; Strano, M. S.; Rogers, J. A. *Nano Lett.* **2004**, *4*, 1643–1647. (c) Bernard, A.; Rernard, J. P.; Renault, J. P.; Michel, B.; Bosshard, H. R.; Delamar, E. *Adv. Mater.* **2000**, *12*, 1067–1070. (d) Cheng, C.-M.; LeDuc, P. R. *J. Am. Chem. Soc.* **2006**, *128*, 12080–12081.
- (7) Lawrence, C. J. *J. Phys. Fluids* **1988**, *31*, 2786–2795 (the temperature in this process is assumed to be constant).

JA072079E